Ab Initio Molecular Orbital Study on the Periodic Trends in Structures and Energies of Hypervalent Compounds: Five-Coordinated XH_5 Species Containing a Group 15 Central Atom (X = P, As, Sb, and Bi)

Jerzy Moc[†] and Keiji Morokuma*[,‡]

Contribution from the Institute for Molecular Science, Myodaiji, Okazaki 444, Japan, Institute of Chemistry, Wroclaw University, F. Joliot-Curie 14, 50-383 Wroclaw, Poland, and Cherry L. Emerson Center for Scientific Computation and Department of Chemistry, Emory University, Atlanta, Georgia 30322

Received May 25, 1995[⊗]

Abstract: An *ab initio* MO study employing effective core potentials (ECP) on central atoms has been carried out for a series of hypervalent XH_5 hydrides, where X = P, As, Sb, and Bi. The $XH_5(D_{3h})$ and $XH_5(C_{4v})$ structures were found to be local minima and transition states (TSs) for Berry pseudorotation, respectively, with barriers of about 2 kcal/mol. All $XH_5(D_{3h})$ are thermodynamically unstable with respect to $XH_3(C_{3v}) + H_2$ by over 40 kcal/mol, and the periodic trend revealed in these stabilities is irregular. The energy decomposition analysis (EDA) was used to study the origin of this irregularity. The TSs for H_2 elimination from $XH_5(D_{3h})$ possessed C_s symmetry and were equatorial−equatorial (eq−eq) for X = P, As, and Sb, whereas zwitterionic axial−equatorial (ax−eq) for X = Bi. The barrier heights to H_2 loss are relatively high and quite similar (30−34 kcal/mol) for all X, and all the XH_5 species are kinetically stable. The all-electron (AE) *ab initio* calculation was also performed for $XH_5(D_{3h})$ and $XH_5(C_{4v})$ with X = P, As, and Sb, showing that the effect of ECP and electron correlation on these structures was minor.

1. Introduction

The hypervalent or hypercoordinate compounds, an intriguing family of chemical species which break (at least seemingly) the octet rule, have attracted considerable attention in both theoretical and experimental studies. On the theoretical side, the models proposed to rationalize the nature of the "hypervalent bond" incorporated the d orbital participation in the hybridization scheme[1] and, later, the formation of the three-center, four-electron bond,[2a,b] without a large contribution of d atomic orbitals.[2c]

The present work is a part of our *ab initio* pseudopotential studies investigating in a systematic manner structures and energies of the closed-shell XH_n and XF_n hypervalent compounds with X = P, As, Sb, and Bi for $n = 4-7$. In the first paper[3] of this series we examined the species with a coordination number n equal to 4, i.e., having formulas XH_4^- and XF_4^-. Extensive mapping of the potential energy surfaces (PES) of the four-coordinated ions[3] revealed that the forms of lowest energy were those of C_{2v} symmetry, whereas their C_{4v} structures were found to be transition states (TSs) connecting C_{2v} minima in the $C_{2v}-C_{4v}-C_{2v}$ pseudorotation. On the other hand, the D_{4h} forms of XH_4^- and PF_4^- appeared to be TSs for inversion of the C_{4v} structures. We also found[3] that the $E(C_{4v}) - E(C_{2v})$ energy differences for both XH_4^- and XF_4^- behaved irregularly on going down the column, whereas the thermodynamic stabilities of $XH_4^-(C_{2v})$ or $XF_4^-(C_{2v})$ with respect to loss of H^- or F^- increased in the order X = P < X = As < X = Sb ≈ X = Bi. The energy decomposition analysis was used to clarify both periodic trends.[3]

Five-coordinated phosphorus compounds are of current theoretical and experimental interest.[4] The prototype phosphorane, PH_5, although not yet observed, has been one of the most extensively studied hypervalent species. The *ab initio* calculations on PH_5[5-7] have centered on the electronic structure, equilibrium geometry, barriers to Berry and "turnstile" pseudorotation processes, and thermodynamic stability with respect to $PH_3 + H_2$; fewer works[5d,e] have concentrated on the barrier height for the H_2 elimination reaction from this species. The related *ab initio* studies investigating substituent effects (i.e. substitution of one or more different ligands for hydrogens in the parent PH_5) on the stabilities of the resultant phosphoranes were also reported.[5a,i,6,8] In this connection we notice the recently proposed conceptions of *equatophilicity*[8] or *equato-*

* To whom correspondence should be addressed at Emory University.
† Institute for Molecular Science and Wroclaw University.
‡ Institute for Molecular Science and Emory University.
⊗ Abstract published in *Advance ACS Abstracts*, November 1, 1995.

(1) (a) Pauling, L. *J. Am. Chem. Soc.* **1931**, *53*, 1367. (b) Pauling, L. *The Nature of the Chemical Bond*, 3rd ed.; Cornell University Press: Ithaca, NY, 1960.

(2) (a) Pimentel, G. C. *J. Chem. Phys.* **1951**, *19*, 446. (b) Rundle, R. E. *J. Am. Chem. Soc.* **1963**, *85*, 112. (c) Kutzelnigg, W. *Angew. Chem., Int. Ed. Engl.* **1984**, *23*, 272.

(3) Moc, J.; Morokuma, K. *Inorg. Chem.* **1994**, *33*, 551.

(4) Holmes, R. R. *Pentacoordinated Phosphorus*: ACS Monograph Series 175 and 176; American Chemical Society: Washington, DC, 1980; Vols. I and II.

(5) (a) Wang, P.; Zhang, Y.; Glaser, R.; Reed, A.; Schleyer, P. v. R.; Streitwieser, A. *J. Am. Chem. Soc.* **1991**, *113*, 55. (b) Wang, P.; Agrafiotis, D. K.; Streitwieser, A.; Schleyer, P.v.R. *J. Chem. Soc., Chem. Commun.* **1990**, 201. (c) Ewig, C. S.; Van Wazer, J. R. *J. Am. Chem. Soc.* **1989**, *111*, 1552. (d) Reed, A. E.; Schleyer, P. v. R. *Chem. Phys. Lett.* **1987**, *133*, 553. (e) Kutzelnigg, W.; Wasilewski, J. *J. Am. Chem. Soc.* **1982**, *104*, 953. (f) Howell, J. M. *J. Am. Chem. Soc.* **1977**, *99*, 7447. (g) Shih, S.-K.; Peyerimhoff, S. D.; Buenker, R. J. *J. Chem. Soc., Faraday Trans. 2* **1979**, *75*, 379. (h) Kutzelnigg, W.; Wallmeier, H; Wasilewski, J. *Theor. Chim. Acta* **1979**, *51*, 261. (i) Keil, F.; Kutzelnigg, W. *J. Am. Chem. Soc.* **1975**, *97*, 3623. (j) Rauk, A.; Allen, L. C.; Mislow, K. *J. Am. Chem. Soc.* **1972**, *94*, 3035.

(6) (a) Wasada, H.; Hirao, K. *J. Am. Chem. Soc.* **1992**, *114*, 16. (b) Wasada, H.; Hirao, K. *Ibid.* **1992**, *114*, 4444.

(7) Trinquier, G.; Daudey, J.-P; Caruana, G.; Madaule, Y. *J. Am. Chem. Soc.* **1984**, *106*, 4794.

0002-7863/95/1517-11790$09.00/0

riphilicity,[6] demonstrating equatorial preference shown by less electronegative ligands or by ligands forming covalent bonds to phosphorus, respectively.

In contrast, almost no attention was devoted in the literature to theoretical studies of the "heavier" analogues of PH_5 containing arsenic (AsH_5), antimony (SbH_5), and bismuth (BiH_5). In recent years, comparative *ab initio* studies on molecular systems including central atoms belonging to a given main group of the periodic table have become possible through the use of pseudopotentials, which can incorporate relativistic effects.[9] As[10,11] in the case of PH_5, there is so far no experimental evidence for the existence of AsH_5, SbH_5, or BiH_5. To our knowledge, AsH_5 has been the subject of one *ab initio* (pseudopotential) study, by Trinquier et al.,[7] whose contribution is also of relevance to our present work. These authors have predicted that a barrier to Berry pseudorotation of AsH_5 is quite similar to that of PH_5 and indicated that AsH_5 is thermodynamically unstable relative to $AsH_3 + H_2$. No vibrational analysis was done for their calculated $AsH_5(D_{3h})$ and $AsH_5(C_{4v})$ structures. When our paper was being revised, the results of recent *ab initio* calculations on the series of period 6 hydrides by Schwerdtfeger et al.[27] were brought to our attention. The latter authors explored relativistic effects on the geometry and thermodynamic stability of BiH_5 with respect to $BiH_3 + H_2$. We have not found in the literature any previous quantum-chemical calculations on SbH_5.

In this paper we report a comparative *ab initio* pseudopotential study for the D_{3h} and C_{4v} structures[22] of the XH_5 hypervalent hydrides, where X = P, As, Sb, and Bi. We have focused on exploring periodic trends in the (i) geometries, (ii) barriers to pseudorotation, and (iii) thermodynamic stabilities of XH_5 relative to $XH_3 + H_2$. Our concern has also been in finding the (iv) energy barriers for the $XH_5 \rightarrow XH_3 + H_2$ decomposition reactions and, thereby, in predicting the possible existence of the XH_5 species. For XH_5 with X = P, As, and Sb, the parallel all-electron (AE) *ab initio* computations were also performed here in order to systematically study the effects of electron correlation on their structures and for the sake of comparison with the *ab initio* pseudopotential findings.

2. Computational Methods

2.1. ECP Calculations. The standard effective core potentials (ECP)[9d] were used for P, As, Sb, and Bi atoms, together with the valence (3s3p2d)/[3s3p2d] basis sets,[9d,12] employed and tested previously.[3] For H, the polarized double-ζ (DZP) basis set of the form (4s1p)/[2s1p] was utilized.[13] The structures were gradient optimized using RHF wave functions (RHF/ECP level) and, for selected cases, with the second-order Møller–Plesset perturbation theory[14a] (MP2/ECP[15] level). Occasionally, UHF wave functions and the UHF based second-order Møller–Plesset perturbation theory and quadratic configuration interaction technique[14c] were employed; these theoretical levels will be referred to as UHF/ECP, UMP2/ECP, and UQCISD/ECP, respectively. The subsequent vibrational frequencies were evaluated numerically using analytical gradients.[16,17] The final correlation energy was computed using Møller–Plesset perturbation theory through fourth order[14b] including triple excitations (MP4SDTQ), but hereafter denoted MP4/ECP.

2.2. AE Calculations. For P, As, and Sb atoms, the (4321/421), (43321/4321/31), and (433321/43321/421) basis sets of Huzinaga et al.[12] were used, respectively, supplemented with two d polarization functions.[12] For H, we employed the DZP basis described above. Geometry optimizations and subsequent frequency calculations were done using both RHF and second-order Møller–Plesset perturbation theory[14a] methods;[16,17] these computational levels will be referred to as RHF/AE and MP2/AE, respectively. The RHF/AE frequencies were computed analytically, whereas the MP2/AE frequencies were evaluated numerically using analytical gradients.

3. Results

3.1. RHF/ECP and MP2/ECP Structures. The D_{3h} structures of XH_5 are found to be minima on the RHF/ECP potential energy surfaces (PES) (with zero imaginary frequencies) for all X (Figure 1). The axial (ax) and equatorial (eq) bond lengths increase gradually from $PH_5(D_{3h})$ to $BiH_5(D_{3h})$, as qualitatively expected from the respective atomic radii of the central atoms.[23] However, the differences between the axial and equatorial distances, Δ(ax–eq), do not show a regular trend. At RHF/ECP, these differences are 0.059, 0.073, 0.066, and 0.084 Å for X = P, As, Sb, and Bi, respectively, thus revealing a smaller value than expected for X = Sb. The MP2/ECP geometry optimization of $XH_5(D_{3h})$ (Figure 1), carried out mainly for the purpose of the $XH_5(D_{3h}) \rightarrow XH_3 + H_2$ decomposition study discussed below, led only to minor changes in comparison with the RHF/ECP findings. Namely, for X = P, As, and Sb, the distances are within 0.006 Å, and for X = Bi, they agree to 0.01 Å. The Δ(ax–eq) values predicted from the MP2/ECP calculation are 0.054, 0.067, 0.059, and 0.072 Å for X = P, As, Sb, and Bi, respectively, thus showing also a "minimum" for X = Sb.

The RHF/ECP C_{4v} structures of XH_5 lie consistently higher in energy than the corresponding D_{3h} forms (Figure 1). A vibrational analysis indicates that the C_{4v} structures are saddle points (one imaginary frequency) for the Berry pseudorotation[11] process (Scheme 1). As expected, the apical (ap) and basal (bas) distances in the C_{4v} structures lengthen gradually on going down the column, whereas the basal hydrogen–central atom–apical hydrogen bond angles tend to widen only slightly in this

(8) (a) Mathieu, S.; Morokuma, K.; Dorigo, A. E. The 1989 International Chemical Congress of Pacific Basin Societies, 1989, PHYS590. (b) Mathieu, S.; Morokuma, K. *Annu. Rev., Inst. Mol. Sci.* **1990**, 18.

(9) (a) Barthelat, J. C.; Durand, Ph.; Serafini, A. *Mol. Phys.* **1977**, *33*, 159. (b) Sakai, Y.; Huzinaga, S. *J. Chem. Phys.* **1982**, *76*, 2552. (c) Krauss, M.; Stevens, W. J. *Annu. Rev. Phys. Chem.* **1984**, *35*, 357. (d) Wadt, W. R.; Hay, P. J. *J. Chem. Phys.* **1985**, *82*, 284. The relativistic mass–velocity and Darwin effects are incorporated in the ECPs for Sb and Bi atoms.

(10) Morokuma, K.; Kitaura, K. In *Chemical Applications of Atomic and Molecular Electrostatic Potentials;* Politzer, P., Truhlar, D. G., Eds.; Plenum Publishing Corp.: New York, 1981.

(11) Berry, R. S. *J. Chem. Phys.* **1960**, *32*, 933.

(12) Huzinaga, S.; Andzelm, J.; Klobukowski, M.; Radzio-Andzelm, E.; Sakaki, Y.; Tatewaki, H. *Gaussian Basis Sets for Molecular Calculations*; Elsevier: New York, 1984. The d polarization exponents employed in the ECP and AE calculations were the same; Cartesian d-type orbitals were used throughout.

(13) Dunning, T. H.; Hay, J. P. In *Modern Theoretical Chemistry;* Schaefer, H. F., III, Ed.; Plenum Press: New York, 1977; Vol. 3, pp 1–27. The p polarization exponent used for H was 0.75.

(14) (a) Pople, J. A.; Binkley, J. S.; Seeger, R. *Int. J. Quantum Chem. Symp.* **1976**, *10*, 1. (b) Krishnan, R.; Frisch, M. J.; Pople, J. A. *J. Chem. Phys.* **1980**, *72*, 4244. (c) Pople, J. A.; Head-Gordon, M.; Raghavachari, J. *J. Chem. Phys.* **1987**, *87*. 5968.

(15) The program used for EDA calculations was IMSPACK (Morokuma, K.; Kato, S.; Kitaura, K.; Ohmine, I.; Sakai, S.; Obara, S. IMS Computer Center Program Library, Institute for Molecular Science, 1980; No. 0372).

(16) Frisch, M. J.; Head-Gordon, M.; Schlegel, H. B.; Raghavachari, K.; Binkley, J. S.; Gonzalez, C.; DeFrees, D. J.; Fox, D. J.; Whiteside, R. A.; Seeger, R.; Melius, C. F.; Baker, J.; Martin. R.; Kahn, L. R.; Stewart, J. J. P.; Fluder, E. M.; Topiol, S.; Pople, J. A. *GAUSSIAN 88;* Gaussian, Inc.: Pittsburgh. PA, 1988.

(17) Frisch, M. J.; Head-Gordon, M.; Trucks, G. W.; Foresman, J. B.; Schlegel, H. B.; Raghavachari, K.; Robb, M.; Binkley, J. S.; Gonzalez, C.; DeFrees, D. J.; Fox, D. J.; Whiteside, R. A.; Seeger, R.; Melius, C. F.; Baker, J.; Martin, R.; Kahn, L. R.; Stewart, J. J. P.; Topiol, S.; Pople, J. A. *GAUSSIAN 90*; Gaussian, Inc.: Pittsburgh, PA, 1990.

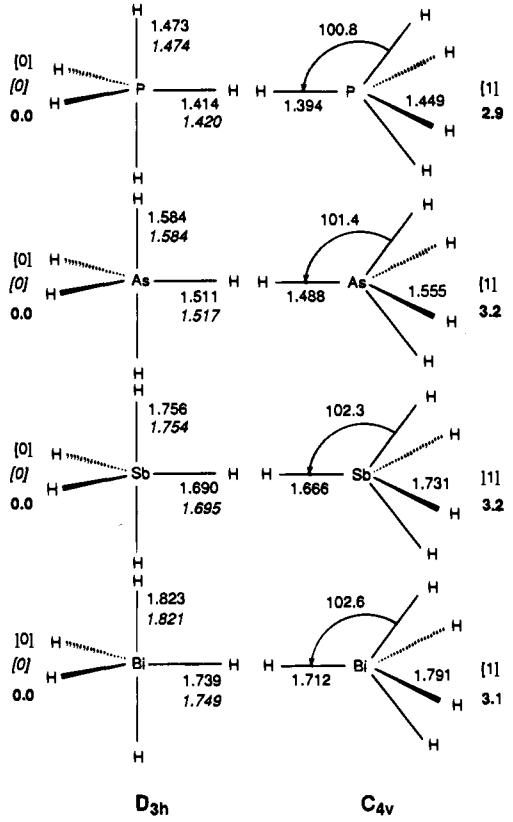

Figure 1. D_{3h} and C_{4v} structures of XH_5 (X = P, As, Sb, and Bi) optimized at the RHF/ECP level (bond lengths in angstroms, bond angles in degrees). Values shown in boldface correspond to RHF energies relative to the D_{3h} structures (kcal/mol); the number of associated imaginary frequencies is given in square brackets. For D_{3h} structures, the MP2/ECP geometrical parameters together with the number of corresponding imaginary frequencies are also shown (in italics).

Scheme 1. Illustration of Berry Pseudorotation for the XH_5 Species (X = P, As, Sb, and Bi) Exchanging the Axial (H1, H3) and Equatorial (H4, H5) Pairs of Ligands through the C_{4v} Transition State

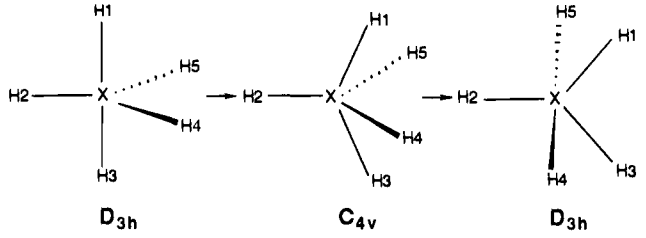

direction (Figure 1). The differences between the basal and apical distances, Δ(bas−ap), are 0.055, 0.067, 0.065, and 0.079 Å, for X = P, As, Sb, and Bi, respectively, thus showing again a relatively small value for X = Sb.

3.2. RHF/AE and MP2/AE Structures. The D_{3h} and C_{4v} structures of XH_5 as found from the RHF/AE and MP2/AE optimizations for X = P, As, and Sb are displayed in Figure 2. A comparison of Figures 1 and 2 reveals that good agreement exists between the RHF/ECP and RHF/AE geometries. That is, for X = P and As, the relevant distances are within 0.005 Å (D_{3h} and C_{4v} forms included), and the bond angles are within 0.2°; for X = Sb, the distances agree to 0.022 Å and the bond angles differ by 0.2°. For $XH_5(D_{3h})$, the MP2/ECP and MP2/AE distances are within 0.013 Å. Thus, as in XH_4^- and XF_4^- studied previously,[3] we found here a good correspondence between the *ab initio* ECP and AE structural predictions for the hypervalent species including P, As, and Sb central atoms.

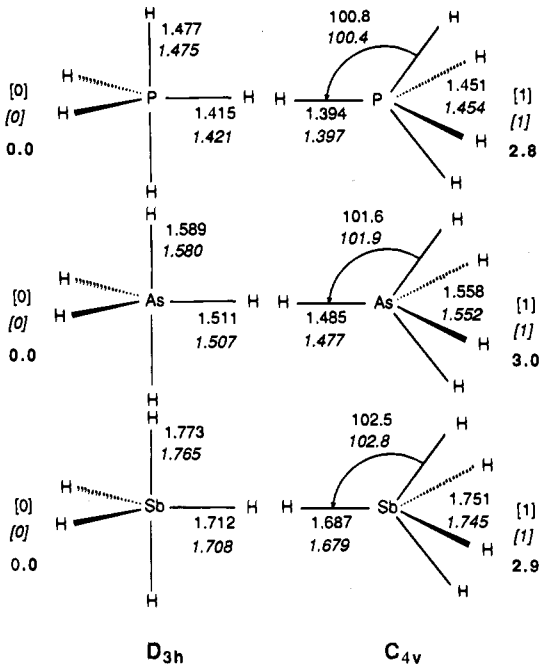

Figure 2. D_{3h} and C_{4v} structures of XH_5 (X = P, As, and Sb) optimized at the RHF/AE and MP2/AE levels (bond lengths in angstroms, bond angles in degrees). Values shown in boldface correspond to RHF energies relative to the D_{3h} structures (kcal/mol); the number of associated imaginary frequencies is given in square brackets. Values in italics are from the MP2 calculation.

The MP2/AE geometry optimizations of the D_{3h} and C_{4v} forms of XH_5 with X = P, As, and Sb (Figure 2) resulted again in minor changes as compared to the RHF/AE structures: the bond lengths are within 0.009 Å, and the bond angles agree to within 0.4°. The minor correlation effects on the axial bond lengths in $XH_5(D_{3h})$ indicate that these bonds have already been described adequately using the RHF wave function. This is in sharp contrast with the XH_4^- hypervalent species, having C_{2v} pseudo-trigonal-bipyramidal structures as the lowest energy structures, where the MP2 correlation effects not only reduced appreciably their axial distances but, for X = P and As, even changed the nature of these species from unstable saddle points to stable minima.[3]

A further inspection of Figures 1 and 2 shows that there is a full agreement between the vibrational analysis results provided by the *ab initio* ECP and AE methods used as far as the number of the corresponding imaginary frequencies is concerned (a complete set of the vibrational frequencies is given in the supporting information).

3.3. Periodic Trend in the Barriers to Berry Pseudorotation. The barrier to Berry pseudorotation of PH_5 has been studied in great detail by *ab initio* MO methods.[5a,b,e,g−j,6,7] The *ab initio* calculations show that the barrier height corresponding to this pseudorotation process (Scheme 1) is quite low: the SCF estimates range from about 2 to about 5 kcal/mol, depending on the basis set used and the geometries assumed. Including electron correlation effects and zero-point energies (ZPE) further reduces this barrier. For instance, Schleyer and co-workers[5a] reported recently the value of 1.1 kcal/mol obtained at the MP4/6-31G(d) + ZPE level.

The periodic trend in the barriers to Berry pseudorotation within the XH_5 series (X = P, As, Sb, and Bi) has not been studied before. As we already noticed from Figures 1 and 2 the RHF/ECP and RHF/AE barriers appeared not to be sensitive to the central atom, being about 3 kcal/mol. The correlation effects at MP4/ECP reduce the barriers by *ca.* 1 kcal/mol for

Table 1. MP2 and MP4 Energy Barriers[a] to Berry Pseudorotation for XH_5 (X = P, As, Sb, and Bi)

species	MP4/ECP[b]	MP2/AE[c]
PH_5	1.9	2.0
AsH_5	2.1	2.2
SbH_5	2.3	2.2
BiH_5	1.9	

[a] In kcal/mol. [b] At the RHF/ECP optimized geometries. [c] At the MP2/AE optimized geometries.

Table 2. Natural Charges for the D_{3h} and C_{4v} Structures of XH_5 (X = P, As, Sb, and Bi) from the RHF/ECP Calculations[a]

species	Q(X)	$Q(H_{ax})$	$Q(H_{eq})$
$PH_5(D_{3h})$	+0.750	−0.248	−0.084
$AsH_5(D_{3h})$	+0.922	−0.285	−0.117
$SbH_5(D_{3h})$	+1.354	−0.352	−0.217
$BiH_5(D_{3h})$	+1.263	−0.341	−0.194
species	Q(X)	$Q(H_{ap})$	$Q(H_{bas})$
$PH_5(C_{4v})$	+0.716	−0.034	−0.170
$AsH_5(C_{4v})$	+0.896	−0.072	−0.206
$SbH_5(C_{4v})$	+1.342	−0.181	−0.290
$BiH_5(C_{4v})$	+1.254	−0.164	−0.272

[a] Subscripts ax, eq, ap, and bas stand for axial, equatorial, apical, and basal, respectively.

all X, and the MP2/AE predictions for X = P, As, and Sb are essentially the same as the MP4/ECP findings (Table 1). Thus, we can conclude that all XH_5 are nonrigid and their Berry pseudorotation barriers are not sensitive to a change of X, being about 2 kcal/mol at our best MP4/ECP level.

3.4. RHF/ECP Natural Charges for $XH_5(D_{3h})$ and $XH_5(C_{4v})$. The RHF/ECP net charges for the D_{3h} and C_{4v} structures of XH_5 computed by using the natural population analysis (NPA)[18] are[19-25] reported in Table 2. For the D_{3h} (C_{4v}) forms, the charge separation between the central atom X and the axial and equatorial (apical and basal) hydrogens increases on going from PH_5 to AsH_5 to SbH_5, and it is actually slightly less for BiH_5 than SbH_5.[26] The negative charges on the hydrogens in $XH_5(D_{3h})$ and $XH_5(C_{4v})$ fall into two groups (see Table 2). The first group includes the XH_5 species with X = P and As, where the negative charges on the axial or equatorial hydrogens in the D_{3h} forms are similar as are those on the apical or basal hydrogens in the C_{4v} forms. The same holds for the second group containing the XH_5 species with X = Sb and Bi. For the D_{3h} structures, the axial hydrogens are more negatively charged than the equatorial ones. This is consistent with the longer (and weaker) axial bonds in comparison with the equatorial bonds. In the C_{4v} structures, the negative charge resides predominantly on the basal hydrogens, which again is in correspondence with the longer basal distances as compared to the apical distances (cf. Figures 1 and 2).

Table 3. Energies of the Reactions $XH_3 + H_2 \rightarrow XH_5$ (X = P, As, Sb, and Bi)[a]

reaction	RHF/ECP[b]	RHF/AE[d]	MP4/ECP[c]	MP2/AE[e]
$PH_3 + H_2 \rightarrow PH_5$	44.8	47.6	45.3	46.7
$AsH_3 + H_2 \rightarrow AsH_5$	55.2	60.9	54.6	58.1
$SbH_3 + H_2 \rightarrow SbH_5$	50.0	45.3	50.2	44.2
$BiH_3 + H_2 \rightarrow BiH_5$	75.4		73.0	

[a] In kcal/mol. [b] The RHF/ECP optimized geometries of XH_3 are (the first entry is the bond length, in angstroms, and the second entry is the bond angle, in degrees), for PH_3, 1.409 and 95.3, for AsH_3, 1.510 and 94.5, for SbH_3, 1.697 and 93.8, and, for BiH_3, 1.759 and 92.5. The RHF/ECP equilibrium distance of H_2 is 0.735 Å. [c] At the RHF/ECP optimized geometries. [d] The RHF/AE optimized geometries of XH_3 are (the first entry is the bond length, in angstroms, and the second entry is the bond angle, in degrees), for PH_3, 1.411 and 95.3, for AsH_3, 1.510 and 94.3, and, for SbH_3, 1.712 and 94.1. [e] At the MP2/AE optimized geometries. The MP2/AE optimized geometries of XH_3 are (the first entry is the bond length, in angstroms, and the second entry is the bond angle, in degrees), for PH_3, 1.415 and 93.6, for AsH_3, 1.504 and 92.4, and, for SbH_3, 1.707 and 92.5. The MP2/AE equilibrium distance of H_2 is 0.739 Å.

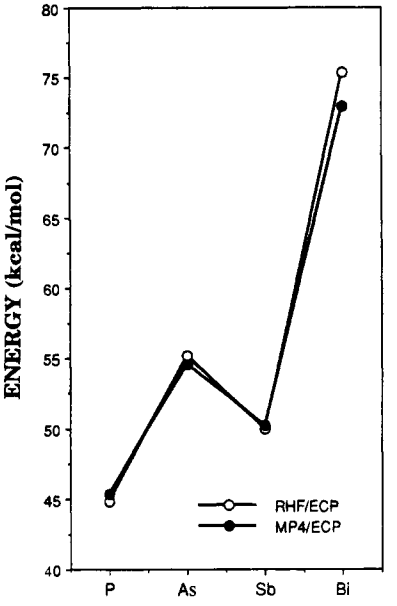

Figure 3. Graphic representation of the $XH_3 + H_2 \rightarrow XH_5$ reaction energies as functions of the central atom X.

3.5. Periodic Trend in the Thermodynamic Stabilities of XH_5 Relative to $XH_3 + H_2$. It has been pointed out previously[5a,c-e,h-j,7] that $PH_5(D_{3h})$ is thermodynamically unstable relative to $PH_3(C_{3v}) + H_2$. In this context an issue of the thermodynamic stabilities of $AsH_5(D_{3h})$, $SbH_5(D_{3h})$, and $BiH_5(D_{3h})$ with respect to H_2 dissociation can be addressed. In particular, a question arises: what is the periodic trend in these stabilities?

In Table 3 the RHF/ECP and MP4/ECP energies of the reactions $XH_3 + H_2 \rightarrow XH_5$ for X = P, As, Sb, and Bi are presented; these energies are also depicted in Figure 3 as functions of X. For X = P, As, and Sb, the corresponding RHF/AE and MP2/AE estimates are given in Table 3 for comparison. The calculations show that, like PH_5, its "heavier" XH_5 analogues with X = As, Sb, and Bi are thermodynamically unstable relative to $XH_3 + H_2$, i.e., at least by over 40 kcal/mol. One also sees that an energy difference between the XH_5

(18) (a) Reed, A. E.; Weinstock, R. B.; Weinhold, F. *J. Chem. Phys.* **1985**, *83*, 735. (b) Foster, J. P.; Weinhold, F. *J. Am. Chem. Soc.* **1980**, *102*, 7211.

(19) Sidgwick, N. V. *The Chemical Elements and Their Compounds*; Clarendon Press: Oxford, 1950; Vol. 1.

(20) Hammond, G. S. *J. Am. Chem. Soc.* **1955**, *77*, 334.

(21) Dai, D.; Balasubramanian, K. *J. Chem. Phys.* **1990**, *93*, 1837.

(22) In analogy to the five-coordinated phosphorus compounds, for which the structures of D_{3h} and C_{4v} symmetry are known to be the fundamental structures, those having the other symmetries have not been explored here.

(23) Slater, J. C. *J. Chem. Phys.* **1964**, *41*, 3199 and references cited therein.

(24) Moc, J.; Dorigo, A. E.; Morokuma, K. *Chem. Phys. Lett.* **1993**, *204*, 65.

(25) For the RHF/ECP equilibrium geometries of the XH_3 and H_2 molecules see footnote *b* in Table 3.

(26) The increasing charge separation between the central atom X and both kinds of hydrogens in the D_{3h} and C_{4v} forms of XH_5 on going from X = P to X = As to X = Sb is expected on the basis of decreasing electronegativities of X in this direction. Namely, according to Pauling's scale (ref 1b) the electronegativity of H is 2.1 and the electronegativities of the central atoms decrease as follows: P (2.1) > As (2.0) > Sb (1.9) = Bi (1.9). The predicted slightly smaller charge separations for the BiH_5 species as compared to the SbH_5 species may have the origin in the "inert pair" effect for the Bi atom. For a discussion of this effect, see ref 19; also see ref 21.

and $XH_3 + H_2$ systems is little affected by electron correlation. Interestingly, the periodic trend revealed in the XH_5 stabilities with respect to H_2 loss is irregular. That is, the endothermicity of the reaction $XH_3 + H_2 \rightarrow XH_5$ increases on going from X = P to X = As, decreases on going from X = As to X = Sb, and then increases sharply with X = Bi (see Figure 3 or Table 3). The large endothermicity of the $BiH_3 + H_2 \rightarrow BiH_5$ reaction of 73 kcal/mol at MP4/ECP compares favorably with the recent prediction by Schwerdtfeger et al. of *ca.* 79 kcal/mol,[27] based[28-33] on the quadratic configuration interaction (QCI) relativistic pseudopotential calculation.

Further examination of the RHF/ECP (MP4/ECP) reaction energies in Table 3 or Figure 3 suggests that the irregularity found is caused by X = Sb, whose central atom does not follow the periodic trend. We also note here that the AE calculations confirm the ECP behavior in the endothermicity in question on passing from X = P to X = As to X = Sb; thus, this is not an artifact of the ECP model.

3.6. Transition State Structures and Barrier Heights for H_2 Elimination from XH_5. The C_s transition state (TS) structures for the $XH_5 \rightarrow XH_3 + H_2$ (X = P, As, Sb, and Bi) decomposition reactions located at the RHF/ECP and MP2/ECP levels are depicted in Figure 4. The RHF/ECP net charges computed at these TSs by using NPA[18] are shown in Figure 5. A vibrational analysis reveals that all the structures in Figure 4 have only one imaginary frequency; thus, they are genuine transition states. The reaction coordinate vectors, corresponding to the imaginary frequencies at each computational level (Figure 6), indicate clearly the TSs found are indeed for elimination of H_2 from $XH_5(D_{3h})$. It is easily seen from Figures 4–6 that two kinds of transition states appear, differing significantly in both geometry and charge distribution.

The first kind involves an elimination of two equatorial (eq) hydrogens, with the $X-H_{eq}$ bonds being broken nearly synchronously (eq−eq elimination). The TSs for the eq−eq elimination were found here for X = P at RHF/ECP and for X = P, As, and Sb at MP2/ECP. The eq−eq TSs can be viewed as distorted C_{2v} structures in which the degree of distortion and the asymmetry of the $X-H_{eq}$ broken bonds increase on passing from X = P to X = As to X = Sb, as does the H−H distance between the departing H atoms (for the trend see the MP2/ECP results in Figure 4). The calculated natural charges (Figure 5) indicate that the eq−eq TSs are only moderately polarized, especially for X = P and As. In particular, the H atoms of the forming H_2 product in these structures bear charges which are close to zero.

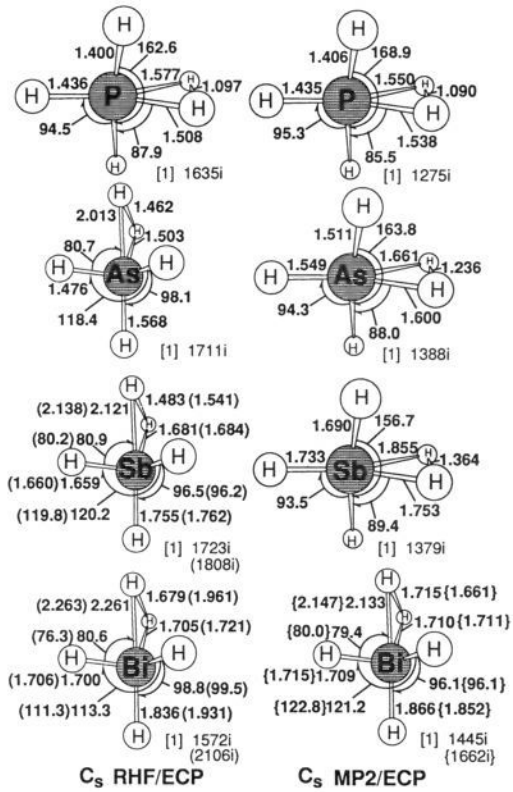

Figure 4. Optimized C_s transition state structures for H_2 elimination from $XH_5(D_{3h})$ (X = P, As, Sb, and Bi) (bond lengths in angstroms, bond angles in degrees). The number of associated imaginary frequencies is given in square brackets followed by the corresponding imaginary frequencies (cm^{-1}). Results are from the RHF/ECP and MP2/ECP calculations unless specified otherwise. Values in parentheses for X = Sb and Bi are from the UHF/ECP calculation, whereas those in curly brackets for X = Bi were obtained at the UQCISD/ECP level.

The TSs of the second kind arise from the elimination of axial (ax) and equatorial hydrogens (ax−eq elimination). The transition state structures corresponding to the ax−eq elimination were found for X = As, Sb, and Bi at RHF/ECP and for X = Bi at MP2/ECP (Figure 4). NPA carried out at the ax−eq TSs reveals that there is a large charge separation between one of the (axial) H atoms of the forming H_2 and the remaining XH_4 fragment (Figure 5). Thus, the TSs for the ax−eq elimination can be described as having zwitterionic $XH_4^+ \cdots H^-$ nature. The salient structural features of the ionic TSs are (i) a very long axial X−H distance involving the departing hydrogen, which increases on going from X = As to X = Sb to X = Bi, and (ii) a relatively long H−H distance of the forming H_2, increasing again in the same direction (for the trends see the RHF/ECP results in Figure 4). We stress here that when the geometry was optimized at the correlated MP2/ECP level, for X = As and Sb, the ax−eq zwitterionic TSs collapsed to the eq−eq ones. On the other hand, our MP2/ECP searches for the eq−eq TS with X = Bi resulted invariably in the ax−eq ionic structure. As a result, at the higher level of theory, the TSs predicted here for H_2 elimination from $XH_5(D_{3h})$ are of the eq−eq type for all X except for X = Bi (see also below).

A possible explanation of the eq−eq TSs emerges in terms of Woodward−Hoffmann rules.[34a] By the same token, for the ax−eq TSs, the stability of the RHF wave functions should be tested.[34b] As a matter of fact, the triplet instability of the RHF/ECP solutions for the ax−eq TSs with X = Sb and Bi was detected here, indicating an existence of the lower energy singlet UHF wave functions for these TSs.[35] Consequently,[36] both TSs

(27) Schwerdtfeger, P.; Heath, G. A.; Dolg, M.; Bennett, M. *J. Am. Chem. Soc.* **1992**, *114*, 7518. The cited energies were estimated from Figure 7 of this work.

(28) The barriers were estimated on the basis of the MP4/ECP energies taken from Tables 3 and 4.

(29) The latter type of selection of the XH_3 and H_2 subsystems was suggested by reviewers.

(30) These authors arrived at the TS having C_{2v} symmetry; however, it was shown later (ref 5d) that the C_{2v} TS had two imaginary frequencies.

(31) This was confirmed in the calculations by Reed and Schleyer (ref 5d).

(32) It was suggested (ref 5e) that in the presence of catalytic amounts of acids the barrier for H_2 abstraction from PH_5 might be decreased significantly.

(33) As previously,[3] one may expect that some of the trends discussed in the present work are influenced by the relativistic contributions from the "heavy" species.[9d] In order to examine computationally the influence of relativistic effects on a given molecular property, it is necessary to compare results of relativistic and nonrelativistic calculations on that property. In fact, Schwerdtfeger et al. found on the basis of the QCI pseudopotential calculations that the relativistic effects substantially decreased the thermodynamic stability of BiH_5 relative to $BiH_3 + H_2$, i.e., by *ca.* 35 kcal/mol.[27]

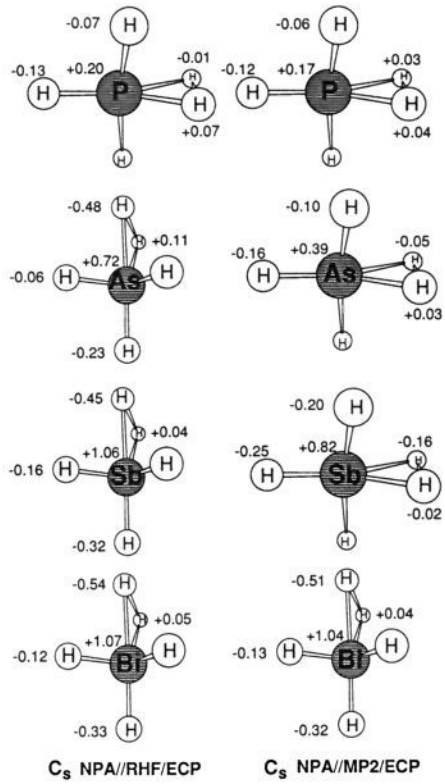

Figure 5. RHF/ECP net charges at the RHF/ECP and MP2/ECP transition states for H_2 elimination from $XH_5(D_{3h})$ (X = P, As, Sb, and Bi) obtained by using the natural population analysis (NPA). The symbol // means at the geometry of.

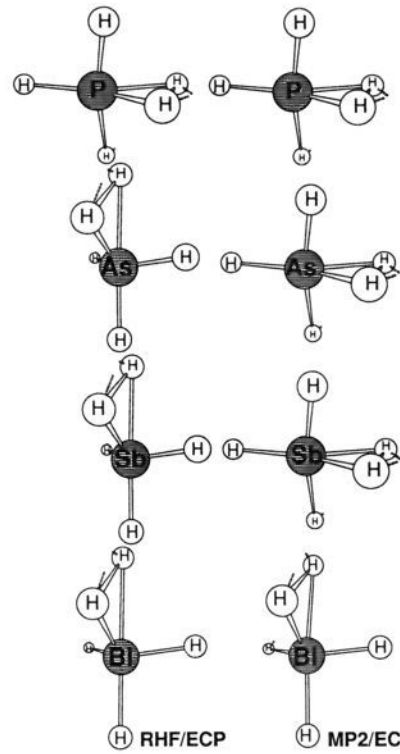

Figure 6. Reaction coordinate vector at the RHF/ECP and MP2/ECP transition states for H_2 elimination from $XH_5(D_{3h})$ (X = P, As, Sb, and Bi). The reaction coordinate vector, i.e., the direction of the normal coordinate corresponding to the imaginary frequency, was calculated at each computational level. The view of structures here is slightly different from that in Figures 4 and 5 for a clearer representation of the vector.

were recalculated at the UHF/ECP level, as shown in Figure 4.[37a] The noticeable structural difference between the RHF/ECP and UHF/ECP predictions is the larger H−H distance of the forming H_2 in the latter case, especially for X = Bi (Figure 4).[38] On the other hand, the concomitant decrease in energy for these TSs is only 0.1 and 1.1 kcal/mol for X = Sb and Bi, respectively (see below). Furthermore, the UMP2/ECP wave functions were used for recalculating the TSs with X = Sb and Bi, which merely reproduced the RMP2/ECP results. Since the TS for X = Bi appeared to be unique among those calculated here, it was important to check this finding at the theoretical level providing a better description of electron correlation than MP2. The UQCISD/ECP wave function was utilized for this purpose, and the resulting TS was also included in Figure 4.[37b] It is seen that, again, the ax−eq type TS was obtained. Moreover, the transition state structures computed for X = Bi at the MP2/ECP and UQCISD/ECP levels are very similar.

To account for the different nature of the TS for X = Bi as compared to those with X = P, As, and Sb found at the correlated level, we recall the results of section 3.5. Namely, the reverse of the reaction $XH_5 \rightarrow XH_3 + H_2$ with X = Bi was indicated to be the most endothermic (73 kcal/mol, Table 3). Thus, one can expect an "early" TS for the highly exothermic $BiH_5 \rightarrow BiH_3 + H_2$ decomposition reaction.[20] Indeed, the ax−eq TS structures resemble much more those of the $XH_5(D_{3h})$ reactants in comparison with the eq−eq TS structures (cf. Figures 1 and 4). On passing, we note that both eq−eq and ax−eq types of transition states were reported recently for H_2 detachment from the MH_4 (M = S, Se, and Te) hypervalent species (see ref 24 for details).

Among the $XH_5 \rightarrow XH_3 + H_2$ decomposition pathways considered, only that with X = P was studied before.[5d,e] Kutzelnigg and Wasilewski,[5e] who extensively investigated the pathway under C_s symmetry, first pointed out the existence of the concerted[30] and zwitterionic transition states at the SCF level, and found that the potential energy surface between the two TSs was very flat. They also obtained very similar barrier heights for H_2 elimination from PH_5 corresponding to both transition states.[31] Interestingly, Kutzelnigg and Wasilewski observed that the zwitterionic TS disappeared when the correlated method was used for geometry optimization[5e] (recall the similar behavior seen above for the TSs with X = As and Sb). Here, at the RHF/ECP level, we have reported only an eq−eq "concerted" TS for X = P. The relevant geometry (Figure 4) compares favorably with the RHF/6-31G(d) one obtained earlier by employing gradient optimization methods,[5d] and it changes somewhat at MP2/ECP (but we did not search for the ax−eq ionic TS for X = P at the RHF/ECP level).

(34) (a) Woodward, R. B.; Hoffmann, R. *Angew. Chem., Int. Ed. Engl.* **1969**, *8*, 781. This explanation has been suggested by a reviewer. More specifically, the [2+2] addition of the lone pair of the XH_3 and H_2 σ bond has to be antarafacial. (b) According to Woodward−Hoffmann rules,[34a] the zwitterionic or biradical TS is predicted for the suprafacial ax−eq approach; the problem of a possible UHF instability of the ionic TSs arises, as pointed out by a reviewer.

(35) The stability calculations[17] revealed the negative eigenvalues of the triplet instability matrices (ref 36) for the RHF/ECP ax−eq TSs with X = Sb (−0.005) and X = Bi (−0.015); the computed values of $\langle S^2 \rangle$ for the resulting singlet UHF/ECP solutions were 0.07 and 0.27, respectively.

(36) Cizek, J.; Paldus, J. *J. Chem. Phys.* **1967**, *47*, 3976.

(37) (a) The values of $\langle S^2 \rangle$ computed for the singlet UHF/ECP wave functions at the UHF/ECP optimized ax−eq TSs with X = Sb and Bi were 0.13 and 0.39, respectively. (b) The corresponding value of $\langle S^2 \rangle$ was found to be 0.20.

(38) When the natural charges were recalculated at the UHF/ECP ax−eq TSs with X = Sb and Bi, and by using the UHF/ECP wave functions, only insignificant changes occurred as compared with the RHF/ECP charges in Figure 5.

Table 4. Barrier Heights for the H_2 Elimination Reactions from $XH_5(D_{3h})$ (X = P, As, Sb, and Bi)[a]

reaction	RHF/ECP	MP2/ECP[c]	MP4/ECP[c,d]
$PH_5 \rightarrow PH_3 + H_2$	45.5	32.6	32.6 (30.2)
$AsH_5 \rightarrow AsH_3 + H_2$	42.8[b]	33.3	32.9 (30.9)
$SbH_5 \rightarrow SbH_3 + H_2$	47.9,[b] 47.8[b,e]	38.1	36.8 (34.9)
$BiH_5 \rightarrow BiH_3 + H_2$	38.5,[b] 37.4[b,e]	34.0[b]	33.5[b] (31.5)[b]

[a] Energies in kcal/mol above the energy of $XH_5(D_{3h})$; the barriers refer to the eq−eq transition states unless noted otherwise. [b] Refers to the ax−eq zwitterionic transition state. [c] At the MP2/ECP geometries. [d] Numbers in parentheses include the zero-point energy (ZPE) correction calculated at the MP2/ECP level. The ZPE values for $XH_5(D_{3h})$ are (kcal/mol), for $PH_5(D_{3h})$, 27.6, for $AsH_5(D_{3h})$, 25.2, for $SbH_5(D_{3h})$, 22.3, and, for $BiH_5(D_{3h})$, 20.7. The ZPE values for the $XH_5(C_s)$ saddle points are (kcal/mol), for $PH_5(C_s)$, 25.2, for $AsH_5(C_s)$, 23.2, for $SbH_5(C_s)$, 20.4, and, for $BiH_5(C_s)$, 18.7. [e] Refers to the UHF/ECP optimized transition state (see the text).

Chart 1. $XH_5(D_{3h})$ (X = P, As, Sb, and Bi) Represented by the $XH_3(D_{3h})\cdots H_{ax}-H_{ax}$ and the $XH_3(C_s)\cdots H_{ax}-H_{eq}$ Interacting Subsystems (Subscripts eq and ax Denote Equatorial and Axial, Respectively)

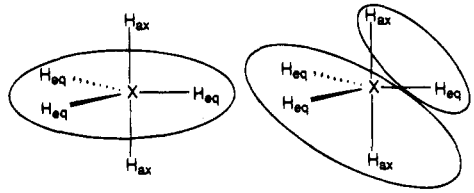

$XH_3(D_{3h})$–H_{ax}-H_{ax} $XH_3(C_s)$–H_{ax}-H_{eq}

The barrier heights for H_2 elimination reactions from $XH_5(D_{3h})$ (X = P, As, Sb, and Bi) predicted at several computational levels are summarized in Table 4. All the energies in Table 4 are relative to the $XH_5(D_{3h})$ reactants. The RHF/ECP, UHF/ECP, and MP2/ECP energies refer to the transition state structures located at each computational level, whereas the MP4/ECP values were computed assuming the MP2/ECP structures. It is seen that, for X = P, As, and Sb, the MP2/ECP energy barriers, referring to the eq−eq TSs, are substantially lower, i.e., by 9.5–12.9 kcal/mol, than the RHF/ECP values. For the reaction with X = Bi, having the ax−eq ionic TS, the MP2/ECP barrier drops only by 4.5 (3.4) kcal/mol with respect to the RHF/ECP (UHF/ECP) finding. On the other hand, all the barriers hardly decrease from MP2/ECP to MP4/ECP. The zero-point energy (ZPE) correction calculated at the MP2/ECP level lowers the barrier heights by 1.9−2.4 kcal/mol. Our best MP4/ECP + ZPE barriers are still relatively high and quite similar for all X, being 30.2, 30.9, 34.9, and 31.5 kcal/mol for X = P, As, Sb, and Bi, respectively. Finally, we notice that, for the eq−eq H_2 elimination from PH_5, our activation barrier of 30.2 kcal/mol agrees well with the correlated (and ZPE corrected) results of earlier calculations of 31.1[5d] and 33.6[5e] kcal/mol (the latter value has been obtained by correcting the original estimate of 36 kcal/mol[5e] for ZPE values given in footnote *d* in Table 4).

4. Discussion

In order to shed more light on the irregularity found in the trend of the thermodynamic stabilities of XH_5 with respect to $XH_3 + H_2$ (section 3.5), an energy decomposition analysis (EDA)[10] was applied at RHF/ECP.[15] The molecular system, "supermolecule", is considered in the EDA method as composed of two interacting subsystems. Here, $XH_5(D_{3h})$ were considered as composed of the XH_3 and H_2 "subsystems". Two different selections of the supermolecules were taken into account (Chart 1): (i) $XH_3(D_{3h})\cdots H_{ax}-H_{ax}$, with the axial hydrogens forming the H_2 subsystem, and (ii) $XH_3(C_s)\cdots H_{ax}-H_{eq}$, where the H_2 subsystem was represented by the axial and equatorial hydrogens.[29]

In the EDA scheme,[10] the binding energy, ΔE, the energy difference between XH_5 and isolated XH_3 and H_2, is divided into two parts, the deformation energy, DEF, and the interaction energy, INT:

$$\Delta E = E(XH_5) - [E(XH_3, \text{equilibrium}) + E(H_2, \text{equilibrium})] = \text{DEF} + \text{INT}$$

DEF is the energy needed to distort both XH_3 and H_2 from their equilibrium geometries[25] to the geometries they take in the $XH_5(D_{3h})$ species:

$$\text{DEF} = [E(XH_3, \text{distorted}) - E(XH_3, \text{equilibrium})] + [E(H_2, \text{distorted}) - E(H_2, \text{equilibrium})]$$

INT is the energy which comes from the interaction of the distorted XH_3 with distorted H_2:

$$\text{INT} = E(XH_5) - [E(XH_3, \text{distorted}) + E(H_2, \text{distorted})]$$

The INT energy can be decomposed into five terms:

$$\text{INT} = \text{ES} + \text{EX} + \text{CTPLX}(H_2 \rightarrow XH_3) + \text{CTPLX}(XH_3 \rightarrow H_2) + R$$

where ES is the electrostatic interaction, EX the exchange repulsion, CTPLX($H_2 \rightarrow XH_3$) the donative interaction from H_2 to XH_3, CTPLX($XH_3 \rightarrow H_2$) the back-donative interaction from XH_3 to H_2, and R the leftover term.

Tables 5 and 6 summarize EDA results for the $XH_5(D_{3h})$ series obtained assuming the $XH_3(D_{3h})\cdots H_{ax}-H_{ax}$ and $XH_3(C_s)\cdots H_{ax}-H_{eq}$ supermolecules, respectively. The energies presented in the left half of both tables were computed at the RHF/ECP geometries and will be discussed first. It is seen that, for all X, the DEF repulsion energies are not counterbalanced by the corresponding INT attraction energies, which leads to the positive, i.e., repulsive, binding energies ΔE. Our purpose now is to reveal the INT energy component(s) responsible for the "extra stability" of SbH_5 over AsH_5, resulting in the irregularity discussed. According to the left half of Table 5, there are two factors responsible for this extra stability: (i) the much smaller exchange repulsive EX term for SbH_5 as compared to AsH_5 and (ii) the larger (more negative) back-donative interaction from XH_3 to H_2, CTPLX($XH_3 \rightarrow H_2$), for X = Sb than X = As. On the other hand, results of the analysis of the $XH_3(C_s)\cdots H_{ax}-H_{eq}$ supermolecules are obscure (see left half of Table 6). That is, the absolute values of all INT components, except for ES, are large and decrease monotonically down a group. For EX and both CTPLX terms, this behavior seems to follow the increase in the distances separating $XH_3(C_s)$ and $H_{ax}-H_{eq}$ subsystems with increasing atomic radius of X (cf. Chart 1).

In order to make a fair comparison of INT components for XH_5 containing different X, especially for the $XH_3(C_s)\cdots H_{ax}-H_{eq}$ supermolecules, we set the EX (repulsive) term approximately constant for all X (i.e., matching the EX of BiH_5).[3] This was achieved by adjusting either the $X-H_{ax}$ distance in $XH_3(D_{3h})\cdots H_{ax}-H_{ax}$ (Chart 1) or the $H_{ax}-H_{eq}$ distance in $XH_3(C_s)\cdots H_{ax}-H_{eq}$ (while keeping the ratio $X-H_{ax}$ distance/$X-H_{eq}$ distance constant, Chart 1). The results of the analysis of such "equal X points"—included in the right side of Tables 5 and 6—indicate consistently that the CTPLX($XH_3 \rightarrow H_2$) term is again more stabilizing for X = Sb than X = As, and thus contributes to the irregularity in question. Additional support for this interpretation comes from a comparison of the ionization potentials (IPs) of both the $XH_3(D_{3h})$ and $XH_3(C_s)$ subsystems,

Table 5. Energy Components for the Interaction between XH_3 and H_2 within the $XH_5(D_{3h})$ Species Assuming the $XH_3(D_{3h})\cdot\cdot\cdot H_{ax}-H_{ax}$ Supermolecule[a]

	D_{3h}[b]				D_{3h}[c]			
	PH_5	AsH_5	SbH_5	BiH_5	PH_5	AsH_5	SbH_5	BiH_5
ΔE	44.8	55.2	50.0	75.4	64.4	63.1	50.0	75.4
DEF	240.6	254.5	271.4	291.0	261.0	265.9	271.1	291.0
INT	−195.8	−199.3	−221.5	−215.6	−196.6	−202.8	−221.1	−215.6
ES	−57.9	−50.1	−42.0	−47.6	−57.7	−54.5	−41.5	−47.6
EX	144.5	99.6	38.9	40.6	40.4	40.4	40.6	40.6
CTPLX($XH_3\rightarrow H_2$)	−129.7	−124.5	−129.4	−125.7	−102.6	−109.1	−130.0	−125.7
CTPLX($H_2\rightarrow XH_3$)	−160.9	−123.5	−79.4	−68.5	−74.0	−74.9	−80.7	−68.5
R	8.2	−0.8	−9.5	−14.4	−2.7	−4.7	−9.4	−14.4

[a] See Chart 1. RHF/ECP energies (kcal/mol) calculated at the RHF/ECP geometries (subscript ax denotes axial). A negative (positive) sign indicates stabilization (destabilization). [b] Within the optimized geometries (cf. Figure 1). [c] The data after setting the EX term approximately constant (see the text).

Table 6. Energy Components for the Interaction between XH_3 and H_2 within the $XH_5(D_{3h})$ Species Assuming the $XH_3(C_s)\cdot\cdot\cdot H_{ax}-H_{eq}$ Supermolecule[a]

	D_{3h}[b]				D_{3h}[c]			
	PH_5	AsH_5	SbH_5	BiH_5	PH_5	AsH_5	SbH_5	BiH_5
ΔE	44.8	55.2	50.0	75.4	84.3	74.3	53.8	75.4
DEF	154.3	166.8	184.0	190.1	207.0	197.1	193.4	190.1
INT	−109.5	−111.6	−134.0	−114.7	−122.7	−122.8	−139.6	−114.7
ES	−28.4	−25.3	−26.4	−33.6	−40.3	−34.6	−30.4	−33.6
EX	585.6	503.4	406.2	341.7	338.1	340.9	343.4	341.7
CTPLX($XH_3\rightarrow H_2$)	−577.8	−518.4	−460.4	−373.4	−335.0	−356.9	−397.7	−373.4
CTPLX($H_2\rightarrow XH_3$)	−537.8	−455.8	−362.3	−262.3	−289.1	−297.3	−304.1	−262.3
R	448.9	384.6	308.9	212.9	203.6	225.2	249.1	212.9

[a] See Chart 1. RHF/ECP energies (kcal/mol) calculated at the RHF/ECP geometries (subscripts ax and eq denote axial and equatorial, respectively). A negative (positive) sign indicates stabilization (destabilization). [b] Within the optimized geometries (cf. Figure 1). [c] The data after setting the EX term approximately constant (see the text).

calculated from Koopmans' theorem (KT). For $XH_3(D_{3h})$, the KT IPs are 8.0, 7.7, 7.0, and 6.7 eV for X = P, As, Sb, and Bi, respectively; the relevant values for $XH_3(C_s)$, put in the same order, are 9.9, 9.6, 9.0, and 9.1 eV. Thus, in both cases, the much lower IP for the subsystem with X = Sb than that for X = As (by 0.6−0.7 eV) makes charge transfer easier for the former central atom.

5. Conclusion

The $XH_5(D_{3h})$ and $XH_5(C_{4v})$ structures were found to be local minima and transition states for Berry pseudorotation, respectively, the corresponding pseudorotation barriers being about 2 kcal/mol. All $XH_5(D_{3h})$ appeared to be thermodynamically unstable with respect to $XH_3(C_{3v}) + H_2$, and the periodic trend revealed in these stabilities was irregular. EDA indicated the more stabilizing back-donative CTPLX($XH_3\rightarrow H_2$) term for X = Sb than X = As as contributing to the irregularity found.[33] The TSs for H_2 elimination from $XH_5(D_{3h})$, optimized at the correlated level, possessed C_s symmetry and were equatorial−equatorial (eq−eq) for X = P, As, and Sb, whereas zwitterionic axial−equatorial (ax−eq) for X = Bi. We related the different nature of the H_2 elimination TS for X = Bi to the high exothermicity (−73 kcal/mol) of the reaction $BiH_5(D_{3h}) \rightarrow BiH_3(C_{3v}) + H_2$. As the computed barrier heights to H_2 loss appeared to be at least 30 kcal/mol above $XH_5(D_{3h})$, all the XH_5 species might be kinetically stable.[32] On the other hand, the isolation of XH_5 based on the $XH_3(C_{3v}) + H_2$ reaction seems to be unrealistic due to the large barriers to overcome of ~75, ~85, ~85, and ~105 kcal/mol for X = P, As, Sb, and Bi, respectively[28] (for X = P, this was also pointed out before[5e]).

Acknowledgment. The present work was performed mainly at the Institute for Molecular Science when both authors were associated with it. Most of the calculations were carried out at the IMS Computer Center. The authors thank Dr. N. Koga for his kind help in carrying out the EDA calculations. J.M. would like to acknowledge the Japan Society for the Promotion of Science for a postdoctoral fellowship.

Supporting Information Available: Tables giving a complete set of total energies obtained from both ECP and AE calculations (3 pages). This material is contained in many libraries on microfiche, immediately follows this article in the microfilm version of the journal, can be ordered from the ACS, and can be downloaded from the Internet; see any current masthead page for ordering information and Internet access instructions.

JA9517126